AN INVESTIGATION INTO THE HEAT AND MASS TRANSFER OF A LIQUID EVAPORATING FROM A CAPILLARY-POROUS BODY

A. V. Luikov and G. V. Vasil'eva

Inzhenerno-Fizicheskii Zhurnal, Vol. 14, No. 3, pp. 395–406, 1968

UDC 536.24:536.423.1

A theoretical analysis is presented for the process of heat and mass transfer in the case of a liquid evaporating from a capillary-porous body into an approaching gas stream. The method of the experimental investigation into this process is described. The excellent agreement between the experimental and theoretical data makes it possible to use the resulting quantitative relationships to calculate the heat-transfer coefficients in the case of intermittent cooling.

The problems of convective heat and mass transfer between a body and the ambient medium are usually solved on the basis of concepts relating to the boundary layer, for which a system of transport equations is derived. It is assumed in this case that the heat transfer between the surface of the body and the medium is described by the so-called law of convection according to which the density of the heat flow q is directly proportional to the temperature head Δt ($\Delta t = t_{med} - t_{sur}$). The proportionality factor is the heat-transfer coefficient α_q. The body-surface temperature t in this case is defined as a function of the coordinate x of the body in the direction of the gas flow ($t_1 = f(x)$). With this method of calculation, the heat-transfer coefficient α_q is independent of the thermophysical characteristics of the body and of its dimensions.

A similar method is used also for the calculation of the mass transfer; here, analogously, a mass-transfer coefficient α_m is introduced, and this quantity represents the proportionality factor between the density of the mass flow j and the concentration difference $\Delta\omega$ or the proportional-pressure difference ΔP.

As demonstrated by research [1], this method is fundamentally incorrect and may be employed as a calculational procedure only for certain special cases of pure heat transfer. A rigorous statement of the problem dealing with the transfer of heat between a body and the ambient medium must be formulated as a conjugacy problem (temperatures and heat flows are equal at the boundary of separation between the solid and the medium) in which the transfer of heat within the body is directly associated with the transfer of heat and mass within the boundary layer at the surface of the body.

The initial attempt to use this approach in solving the problem of the transfer of heat between a moist body and the flow of a heated gas is described in [2]. Here it is quite natural that a number of simplifications and assumptions were adopted. It was assumed that the evaporation of the liquid takes place within the body, at a surface removed from the surface of the body by a distance ξ. The surface evaporation temperature t_e is assumed to be a constant and equal to the temperature of the wet-bulb thermometer ($t_e = t_M$). However, this last restriction does not apply to the constant quantity (t_{sur} = const). It is then assumed that the linear velocities of motion in the boundary layer are constant ($\bar{w}_x$ = const = $5/8\bar{w}_{med}$; $\bar{w}_y$ = const). This assumption was necessary to solve the differential equation of heat transfer for the boundary layer. As a result, it was established that the relative coefficient of heat transfer or, more exactly, the Nusselt number, is a function not only of the hydrodynamics of the flow (the Re number) and its physical characteristics (the Pr number), but also of the thermophysical properties of the body (the coefficient of thermal conductivity λ_{sol} of the body) and of the location of the evaporation surface ξ. These characteristics of the body are incorporated into the generalized argument K:

$$K = \frac{Hx}{\sqrt{\overline{Pe}_x}} = \frac{\lambda_m x}{\lambda \xi} \overline{Pe}_x^{-0.5}. \quad (1)$$

The local Nusselt number Nu_x is thus a function of three numbers:

$$Nu_x = f(Re_x, Pr, K). \quad (2)$$

This is the basic difference in the solution of the problem of heat transfer between a body and the ambient medium, as opposed to the generally accepted calculational procedure based on the law of convective heat transfer. Despite the number of simplifications, this method of solution yields fairly accurate results.

Let us dwell on this in somewhat greater detail. The differential equation of transfer in the boundary layer for laminar streamlining of a flat plate has the form

$$w_x \frac{\partial t(x, y)}{\partial x} + w_y \frac{\partial t(x, y)}{\partial y} = a \frac{\partial^2 t(x, y)}{\partial y^2}, \quad (3)$$

where w_x and w_y are components of the velocity of motion along and across the flow, respectively.

For the calculational procedure we will assume that $w_x = \bar{w}_x$ = const and $w_y = \bar{w}_y$ = const, in which case, as demonstrated in [2], we will have

$$Nu_x = \frac{\alpha_x x}{\lambda} =$$

$$= \frac{1}{\sqrt{\pi}} Pr^{0.5} \sqrt{\overline{Re}_x} \left[\exp\left(-\frac{B}{4}\right)^2 - \frac{\sqrt{\pi}}{2} \times \right.$$

$$\left. \times B \operatorname{erfc}\left(\frac{1}{2} B\right) \right], \quad (4)$$

where $Re_x = w_x x/\nu$ is the local Reynolds number for the averaged flow velocity w_x in the boundary layer;

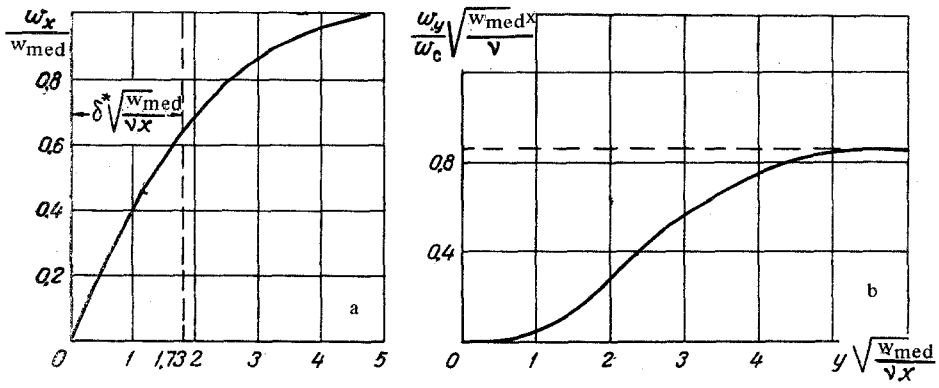

Fig. 1. Profiles of longitudinal w_x(a) and transversal w_y(b) velocity when flat plate is in laminar flow.

Table 1

The Quantity N(B) for Various Values of B

B	N (B)	B	N (B)	B	N (B)	B	N (B)
0	1	0.30	0.7565	0.06	0.9478	0.80	0.4469
0.01	0.9912	0.40	0.6852	0.08	0.9307	1.00	0.3538
0.02	0.9825	0.50	0.6188	0.10	0.9139	2.00	0.0891
0.04	0.9653	0.60	0.5570	0.20	0.8327	5.00	0.0001

Table 2

Theoretical Values of N as a Function of K and B

K	$\frac{1}{K}$	N (K, B)						
		B = 0	B = 0.04	B = 0.08	B = 0.2	B = 0.4	B = 0.6	B = 1
	0	1	1	1	1	1	1	1
10	0.1	1.06	1.06	1.06	1.075	1.08	1.11	1.13
8	0.125	1.08	1.08	1.08	1.10	1.11	1.13	1.175
6	0.166	1.103	1.10	1.11	1.15	1.15	1.18	1.24
5	0.200	1.104	1.11	1.11	1.12	1.16	1.18	1.29
4	0.250	1.24	1.111	1.12	1.152	1.18	1.20	1.30
3	0.333	1.16	1.145	1.17	1.19	1.23	1.27	1.40
2	0.500	1.22	1.20	1.22	1.21	1.33	1.38	1.57
45	0.68	1.26	1.25	1.28	1.32	—	1.49	1.72
1	1.0	1.32	1.325	1.35	1.39	1.50	1.61	1.94
0.8	1.25	1.36	1.355	1.39	1.45	1.56	1.69	2.05
0.6	1.66	1.40	1.40	1.43	1.50	1.66	1.76	2.22
0.4	2.5	1.44	1.44	1.48	1.56	1.70	1.88	2.40
0.2	5.0	1.50	1.51	1.55	1.63	1.80	2.00	2.62
0.1	10	1.53	1.54	1.58	1.69	1.86	2.09	2.76

$B = w_y/w_x(Re_x)^{-0.5}$ is a dimensionless parameter characterizing the transfer in the transverse direction.

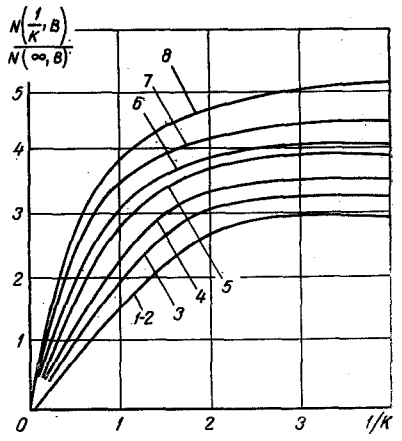

Fig. 2. N(K, B) versus 1/K.

If we adopt the parabolic law $w_x(y)$ for the velocity distribution along the coordinate y, we have $w_x = (5/8)w_{med}$, where w_{med} is the velocity in the core of the flow. The average value of w_y is determined from Fig. 1b from the magnitude of the parameter $(y/x)Re$. For the average value of $w_x/w_{med} = 5/8$ the quantity $\delta^*(w_{med}/\nu x)^{1/2} = 1.73$ (see Fig. 1a). This average value of $y(w_{med}/\nu x)^{1/2} = 1.73$ corresponds to $(w_y/w_a)(w_a x/\nu)^{1/2} = 0.2$ (see Fig. 1b). Hence we have

$$B = \frac{\bar{w}_y}{w_x}\sqrt{\overline{Re}_x Pr} = \frac{\bar{w}_y}{w_{med}}\sqrt{\frac{w_{med}x}{\nu}}\sqrt{\frac{8}{5}Pr} =$$

$$= 0.2 \cdot 1.26 \cdot 0.838 = 0.21. \quad (5)$$

Here it was assumed that Pr = 0.7, which corresponds to the values of the Prandtl numbers for air. When B = 0.21, the expression in the brackets of formula (4) is equal to 0.84. Consequently, for air (Pr = 0.7)

$$Nu_x = \frac{1}{\sqrt{\pi}}\sqrt{Pr}\sqrt{\overline{Re}_x}\,0.84 = 0.31\sqrt{\overline{Re}_x}, \quad (6)$$

which is virtually coincident with the empirical formula for the local Nusselt number Nu_x in the case of laminar streamlining of a flat plate

$$Nu_x = 0.30\sqrt{\overline{Re}_x}. \quad (7)$$

It follows from formula (4) that with an increase in the parameter B the Nusselt number diminishes. We will denote the expression in brackets by N(B):

$$N(B) = \frac{Nu_x\sqrt{\pi}}{\sqrt{Pr\,\overline{Re}_x}} =$$

$$= \left[\exp\left(-\frac{1}{4}B^2\right) - \frac{1}{2}\sqrt{\pi}\,B\,\mathrm{erfc}\left(\frac{1}{2}B\right)\right]. \quad (8)$$

The function N(B) is shown for various values in Table 1. We see from the table that when $B \geq 5$ the quantity N(B) is very small and, consequently, the Nu_x number is virtually equal to zero. Formula (4) will also be valid in the case of injection into the boundary layer through the porous surface of the body. In this case, the parameter B is given by [3]

$$B = \sqrt{Pr\,\overline{Re}_x}\,\frac{1}{\bar{w}_x}\left[\bar{w}_y + w_s\left(\frac{c_1 - c_2}{c_1}\right)\right], \quad (9)$$

where w_s is the linear velocity of injection at the body surface; c_1 and c_2 are, respectively, the specific heat capacities of the flow and of the injected gas.

With an increase in the injection velocity w_s we thus have an increase in the parameter B, as a result of which the Nusselt number diminishes in accordance with formula (4). This is explained by the thickening of the boundary layer, resulting in a change in the temperature profile in the boundary layer. Some investigators use formula (4) to calculate the heat transfer in the evaporation of a liquid from porous bodies, assuming the process of intermittant evaporation to be analogous to the process of gas injection into the boundary layer. As demonstrated by the calculations, with an evaporation intensity lower than 25 kg/m^2 · hr, the linear rate of evaporation is independent and has no effect on the magnitude of the parameter B [3]. Moreover, it should be borne in mind that the linear rate of evaporation (in terms of its physical significance) is not the velocity of molar motion, but characterizes the diffusion of the vapor in the boundary layer. The injection velocity w_s and the linear rate of evaporation are therefore quantities which are different in their physical nature, although expressed in the same units.

The quantitative relationships governing the heat and mass transfer in the case of injection into the boundary layer cannot thus be used to analyze the processes of heat and mass transfer for the evaporation of a liquid from a porous body.

In the case of transpiration cooling, as in the case of drying, the evaporation of the liquid, in the majority of cases does not take place at the surface, but at some depth ξ from the body surface. In the evaporation zone $(0, -\xi)$ we have evaporation of the liquid, with the moisture being transported primarily in the form of vapor. Unlike reference [2], the temperature profile in the evaporation zone is therefore assumed in the form of the relationship

$$t(x, y) = t_e + f(x)\{1 - \exp[-D(y + \xi)]\}, \quad (10)$$

where $f(x)$ is a function by means of which we take into consideration the variation in temperature along the coordinate x; D is a constant; t_e is the evaporation temperature.

The boundary conditions have the form

$$-\lambda\frac{\partial t(x, 0)}{\partial y} = -\lambda_{sol} f(x) D \exp^{-D\xi} \quad (11)$$

or, using formula (10),

$$-\lambda\frac{\partial t(x, 0)}{\partial y} =$$

$$= -\lambda_{sol}[t(x, 0) - t_e]\frac{D}{\exp D\xi - 1}, \quad (12)$$

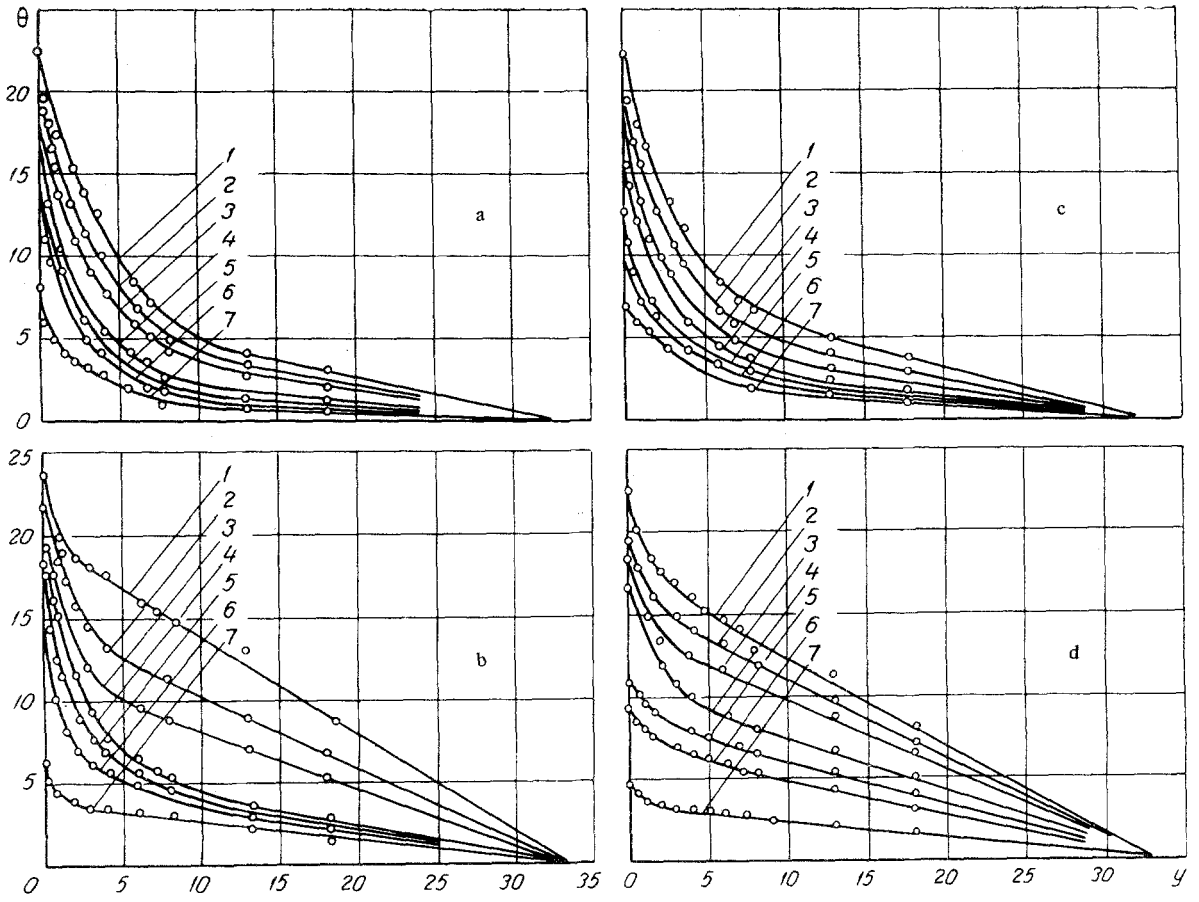

Fig. 3. Profiles of temperature distribution in quartz sand 1, 2, 3, 4, 5, 6, and 7) thickness of dry interlayer equal to 0, 2, 3, 4, 5, 6 and 8 mm, respectively ; a) porosity 35 percent; b) porosity 36 percent; c) 38 percent; d) 42 percent.

Table 3

Experimental Values of K and N(K, B) for Sands Exhibiting Various Porosities (B = 0.2)

$\xi \cdot 10^3$	H	K	$\frac{1}{K}$	$N(K, B)$	$N(\infty, B)$	$\frac{N(K, B)}{N(\infty, B)}$
			Porosity *42* %			
8	624	0.509	1.965	1.2745	0.8327	1.53
6	835	0.681	1.468	1.2353		1.48
5	1000	0.816	1.225	1.2051		1.447
4	1240	1.01	0.99	1.1695		1.4
2	3760	3.07	0.326	0.9948		1.138
			Porosity *38* %			
8	444.25	0.363	2.75	1.3003	0.8327	1.56
6	587.9	0.480	2.08	1.2811		1.538
5	721.9	0.589	1.697	1.2488		1.499
4	906.02	0.739	1.353	1.2252		1.47
2	1815.6	1.482	0.675	1.1011		1.322
			Porosity *36* %			
8	677.3	0.553	1.808	1.2633	0.8327	1.516
6	914.6	0.746	1. 34	1.2211		1.465
5	1076.05	0.878	1.138	1.19025		1.429
4	1335.5	1.09	0.917	1.1694		1.404
2	2781.1	2.27	0. 44	1.0332		1.24
			Porosity *35* %			
8	771.2	0.629	1.589	1.24882	0.8327	1.499
6	1010.6	0.825	1.212	1.2058		1.447
5	1199.7	0.979	1.021	1.1695		1.404
4	1488.9	1.215	0.823	1.1308		1.357
2	2872.3	2.344	10.427	1.0281		1.234

where λ_{sol} is the thermal conductivity of the body in the evaporation zone. Boundary condition (2) is thus

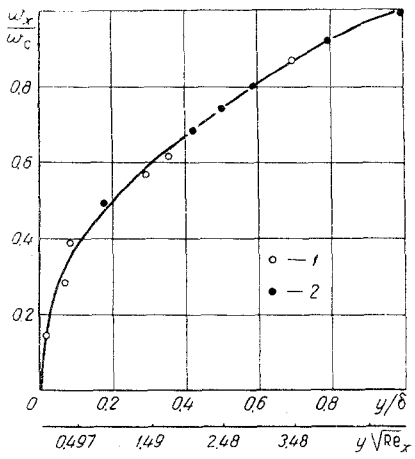

Fig. 4. Profile of velocity distribution $w_x(y)$ in air boundary layer: 1) experimental points; 2) theoretical values.

similar to the condition cited in reference [2], but the quantity H in this case is given by

$$H = \frac{\lambda_{sol}}{\lambda} \frac{D}{[\exp D\xi - 1]}. \quad (13)$$

The remaining boundary conditions remain as before, i.e., when

$$y = -\xi \quad t(x, -\xi) = \bar{t}_e = \text{const}. \quad (14)$$

For the given boundary conditions we obtain a solution for the differential equation (3) that is analogous to the solution given in [2].

Consequently, the local Nusselt number will be given by

$$Nu_x = \frac{x}{t_{med} - t(0, x)} \frac{\partial t(0, x)}{\partial y} =$$

$$= \frac{1}{\sqrt{\pi}} \sqrt{Pe_x}\, N(K, B), \quad (15)$$

where N(K, B) is a function which is given by

$$N(K, B) = \left[\varphi(K, B) - \frac{1}{2}\sqrt{\pi}\, B \operatorname{erfc} \frac{1}{2} B\right] \times$$

$$\times \left[\left(1 - \frac{B}{K}\right) - \frac{1}{K\sqrt{\pi}} \varphi(K, B) + \right.$$

$$\left. + \frac{1}{2} \frac{B}{K} \operatorname{erfc} \frac{1}{2} B\right]^{-1} \quad (16)$$

$$\varphi(K, B) = \left(1 - \frac{1}{2} \frac{B}{K}\right) \times$$

$$\times \sqrt{\pi}\, K \exp(K^2 - BK) \operatorname{erfc}\left(K - \frac{1}{2} B\right). \quad (17)$$

The quantity K characterizes the influence of the penetration of the evaporation zone. It is given by

$$K = \frac{\lambda_T D}{\lambda(\exp D\xi - 1)} \sqrt{Pe_x}. \quad (18)$$

The curves of N'(K, B) were plotted for various values of B from formula (16) (see Fig. 2 and Table 2). We see from Fig. 2 that with a reduction in 1/K the quantity N'(K, B) diminishes, i.e., with greater penetration of the evaporation surface the Nu_X number increases. The greater the value of B the more intensive the reduction in Nu_X. The analytically derived relationships have subsequently been confirmed by experiment.

The experimental investigation was carried out in a continuous-action wind tunnel with an enclosed working section exhibiting the following airstream parameters: velocity, 5 m/sec; temperature, 353° K; humidity, 5%. The model—a box made of plastic and filled with quartz sand—was positioned within the working section of the tunnel.

During the course of the experiment we studied the effect of a dry layer of sand on the heat-transfer coefficient (the thickness of the layer was varied as follows: 0, 2, 4, 5, 6, and 8 mm, with various dispersion ratios—quartz-sand porosities of 35, 36, 38, and 42%.

When we use natural material we cannot expect a completely flat rectilinear boundary of phase transition. This is possible only through resort to articicial means. In particular, in our experiments the dry layer

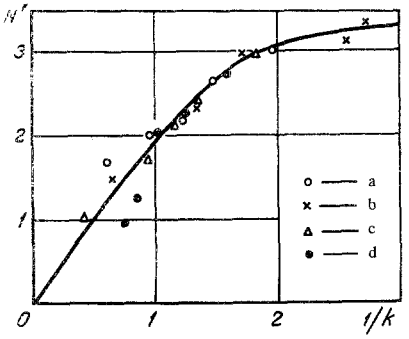

Fig. 5. Experimental data compared to theoretical curve: a) porosity 42 percent; b) 38 percent; c) 36 percent; d) 35 percent.

was achieved by applying a very fine hydrophobic film to the sand grains. The sand was poured into the rectangular box. Water was fed into the box from below through a connecting tube. To ensure uniform entry of the water, an additional supporting grid was installed inside the box, and the sand was poured directly onto this grid. The space between the bottom of the box and the grid was filled with water which was uniformly drawn up by the sand until it reached the top layer which had been treated with the hydrophobic film. To avoid "parasite" unanticipated heat losses through the side walls, the latter were carefully insulated with a layer of foam plastic. In addition, the box was fitted out with a thermostating jacket in which water was

continuously circulated at a specific temperature. The bottom wall of the measuring unit was made of massive textolite. A rectangular hole was cut into its center to house a box exhibiting dimensions of 260 × 140 mm. To produce a hydrodynamic pattern similar to the one prevailing under conditions of the external streamlining of a plate, provision was made for the evacuation of air in front of the box. The model was mounted in a positioning device and set flush with the bottom wall of the working section of the tunnel. This procedure eliminated the distorting effect of tunnel-wall vibrations.

VTK-500 scales were used to measure the amount of moisture being vaporized during the course of the experiment, and in addition we measured the temperature of the sand, the flow, the walls of the box, and of the water entering the box. Particular attention was devoted to the accuracy with which the temperature fields were measured in the sand. For this purpose, we fabricated a 17-junction differential thermocouple made of copper-constantan wire; the junction diameter was 0.15–0.2 mm. The junctions of the differential thermocouple were positioned along the vertical, with variable space (0.4 mm near the outside surface of the sand and up to 1 mm at some distance from the surface). We used a PMS-48 potentiometer to measure the thermal emf of the thermocouples, and this device was fitted out with a sensitive M-17-1 galvanometer. To investigate the hydrodynamic boundary layer we used a miniaturized Pitot tube with an effective center height of 0.15 mm, which was moved in the vertical plane by means of a miniaturized positioning device.

As a result of this experiment we were able to plot the temperature profiles in the sand and the velocity distribution in the boundary layer. In addition, we measured the quantity of evaporated moisture. Figure 3 shows the curves for the temperature distribution in dry and moist sand (moisture content, 100%). We see from these graphs that all of the temperature-distribution curves exhibit three characteristic segments.

The first segment is the penetration zone ($0 > y > -\xi$). It is in this segment that the heat is transmitted by conduction (natural convection and radiation are neglected). The heat is expended on phase conversion, and a fraction of the heat is spent on heating the sand. It is in this segment that the temperature profile is presented in the form of a curve. If there were no evaporation, the temperature distribution would be linear in nature. However, the presence of mass flow distorts the temperature profile; this segment is well-approximated by formula (10).

The second segment is the transition zone. It is here that we have a qualitative change in the pattern, since it is in this segment that liquid is evaporated. In this connection, it should be borne in mind that the moisture is not evaporated on a plane which is parallel to the outside contour of the body, but at some layer of finite dimensions. The phenomenon of volume evaporation was also noted in [4], and it was found here that the intensive evaporation which occurs in drying takes place in a very thin layer at the boundary of phase separation. Consequently, we must assume that t_e = = const in the solution, this being the average temperature through the thickness of the evaporation zone.

The third segment is the zone of moist sand (φ = = 100%). There is no evaporation; however, a portion of the heat is spent on heating the sand. The heat is transmitted by the conduction of the skeleton, so that the temperature profile in this segment of the curves is shown in the form of a straight line. This fact indicates that the thickness and structural characteristics of the dry interlayer of the porous body exert considerable influence on the intensity of mass transfer during the course of evaporation from the capillary-porous body. If the intensity of evaporation were independent of the structural characteristics of the topmost dry layer, it might be possible to set up adiabatic conditions and to eliminate the heating of the wet sand. The dry interlayer forms a major thermal resistance which prevents a removal of moisture, such that all of the heat not spent on phase conversion would be removed by the vapor into the flow. In actual practice we find that adiabatic evaporation is a special case which can be achieved only within thin interlayers or by choosing a particular porosity for the interlayer.

Analysis of the experimental curves shows that with increasing depth for the phase-transition zone the curves move higher and higher, retaining all the features of their shape. As the dry interlayer thickens, there is an increase in the hydraulic resistance of the porous structure. At the same time, the pressure within the porous material increases and, consequently, the evaporation temperature of the moisture rises. For small penetrations the evaporation temperature for the surface is therefore independent of the magnitude of penetration and it is equal throughout to the temperature of the wet-bulb thermometer, which is a function of the external conditions. With increasing thickness for the dry interlayer, the evaporation temperature rises. Consequently, we have to introduce boundary conditions into the solution to take into consideration the variation in temperature as a function of the thickness ξ.

To determine the dimensionless complex B characterizing the transfer of heat in the lateral direction we plotted the velocity distribution profile of $w_x(y)$ in the boundary layer (Fig. 4). The excellent agreement between the results of the theoretical Blasius solution for a plate of infinite length ($l \to \infty$) with the experimentally derived data suggests the possibility of using the "pure" heat-transfer data—uncomplicated by mass transfer—for the calculational scheme. The linear rate of evaporation (the magnitude of the Stefan flow) is determined from the formula.

$$w_{xy} = -\frac{D_{12}}{(1-\rho_{10})}\nabla\rho_{10} = \frac{j_{sur}}{\rho}, \qquad (19)$$

where j_{sur} is the mass flow rate of the evaporating moisture; ρ_1 is the vapor concentration; ρ is the den-

sity of the moist air; ρ_{10} is the relative concentration of the vapor; and D_{12} is the coefficient of vapor diffusion in the air. Formula (18) was used to calculate the value of K for sands of various porosities as a function of the thickness of the dry interlayer (Table 3). We see from Table 3 that the value of K diminishes as the thickness of the dry interlayer increases. It is difficult to establish a clear quantitative relationship between K and the porosity of the sand, since the sand is a natural material which involves various particle shapes. During the course of the experiment, the sands were chosen by screening the particle dimensions. However, the porosity of disperse materials is determined primarily by the manner in which the particles are packed, and depending on the manner in which the sand was poured, the porosity varied within a defined range from experiment to experiment. However, it is possible to achieve a qualitative evaluation: with an increase in the porosity of the sand, the value of K diminishes. This is explained by the change in the effective thermal conductivity of the porous dry interlayer (the thermal conductivity of the skeleton increases as its porosity diminishes, since a greater portion of the porous body is occupied by its skeleton in this case —the skeleton exhibiting a considerably greater coefficient of thermal conductivity than the pore space filled with the water vapor).

Knowing the values of $K = f(\xi, \text{sur})$ and B (B = 0.2), we can find the values of N(K, B). Figure 5 shows the theoretical curve of $N = f(K)$ for B = 0.2 and the experimental points for quartz sand with various porosities (35, 36, 38, 42%).

We can see from these graphs that the experimental data line up rather well along the theoretical curve. Only the very thin interlayers (ξ = 2 mm) represent an exception; here we note a certain deviation from the theoretical data, which can be explained by the difficulties encountered in measuring temperatures in the very thin interlayers. Consequently, the experiment confirms the proposed theoretical solution.

In conclusion, let us dwell on the work of Morgan and Jerazunis [5], who investigated the effect of heat and mass transfer. These authors attempted to analyze the heat and mass transfer occurring on vaporation of a liquid from porous bodies (evaporation cooling) as well as during the process of drying. First of all, it should be noted that the process of drying moist bodies is a typical nonsteady process of heat and mass transfer, while the process of evaporation cooling is a steady-state process. For nonsteady heat- and mass-transfer processes, the quantitative relationships governing steady heat and mass transfer are not suitable. In particular, the so-called formula of convective heat transfer ($q = \alpha \Delta t$) cannot be used, since the heat-transfer coefficient α is a function of both time and of the thermophysical characteristics of the body. Equally unsuitable is the Dalton formula for mass transfer during a period of a declining drying rate.

So far as the analysis of heat- and mass-transfer processes is concerned in the event of transpiration cooling, the original relationships given by these authors exhibit a fundamental error in our opinion. Initially the authors assume that the intensity of the heat and mass transfer on evaporation of the liquid from the porous body is described by the relationships from the classical theory of heat and mass transfer in which the effects of the penetration of the evaporation surface into the body is not taken into consideration. In particular, the authors base their calculations on relationships according to which the heat- and mass-transfer coefficients are determined from the generally accepted formulas of external heat and mass transfer:

$$\mathrm{Nu}_x = A_1 \mathrm{Re}^n \mathrm{Pr}^\rho, \quad \mathrm{Nu}_{xm} = A_2 \mathrm{Re}^n \mathrm{Pr}_m^\rho, \tag{20}$$

where A_1 and A_2 are constants, and ρ and n are exponents.

However, as was demonstrated earlier, these formulas lose validity when the evaporation zone is set deeper into the body.

In addition, they adopted an unjustified assumption to the effect thatthe heat- and mass-transfer coefficients vary as functions the coordinate x and of thickness ξ in accordance with the formula

$$\frac{\alpha(x, \xi)}{\alpha_0} = \frac{\alpha_m(x, \xi)}{\alpha_{m_0}} \left[1 - \left(\frac{\xi}{x}\right)^\gamma\right]^{-\beta}, \tag{21}$$

where γ and β are constants; α_0 and α_{m0} are, respectively, the coefficients of heat- and mass-transfer without penetration of the evaporation surface. On the basis of these formulas, the authors carry out the calculation and, quite naturally, attain results exceeding our data by a factor of three. The relationship between the heat- and mass-transfer coefficients and the Re and Pr numbers—as well as the coordinates x and ξ—must be derived from the solution of the conjugacy problem rather than being assumed in advance in the form of empirical formulas. Thus the study carried out in [5] once again confirms the inapplicability of conventional methods of calculating heat transfer in connection with the problem of transpiration cooling.

The basic conclusion of our paper is the fact that in order to determine both the quantitative and qualitative pattern of the effect exerted by mass transfer on heat transfer, we have to take into consideration the hydrodynamic conditions of body streamlining (external conditions) and the properties of the capillary-porous body (internal conditions). Consequently, the transfer of heat and mass between capillary-porous bodies and the ambient medium is a single interrelated heat- and mass-transfer process which takes place in the boundary layer of the body and in the boundary layer of the medium.

NOTATION

t is the temperature; q is the specific heat flux; α_q is the heat transfer coefficient; α_m is the mass transfer coefficient; λ is the thermal conductivity; a is the thermal diffusivity; w is the velocity; φ is the

humidity; ω is the concentration; j is the mass flow density; P is the pressure; ξ is the distance; x and y are coordinates; c is the specific heat capacity; δ^* is the conventional depth of boundary layer. Similarity criteria: Nu_x is the local Nusselt number; Pe_x is the local Peclet number; $\overline{Pe}_x$ is the local Peclet number based on mean integral velocity in boundary layer; Pr is the Prandtl number. Subscripts: med is the ambient medium (humid air), w(wet bulb) is the state of adiabatic saturation; sur is the surface; sol is the solid; x is the local value which depends on the coordinate; e is the evaporation surface.

REFERENCES

1. A. V. Luikov and T. L. Perel'man, Heat and Mass Transfer Between Solids and an Ambient Gaseous Medium [in Russian], Izd. Nauka i tekhnika, 1965.

2. A. V. Luikov, IFZh, no. 11, 1962.

3. A. V. Luikov, Int. J. Heat Mass Transfer, **6**, 559–570, 1963.

4. A. H. Nisson, H. H. George, and T. V. Bolles, A.I.Ch.E. Journal, **6**, 406–410, 1960.

5. R. Morgan and S. Jerazunis, A.I.Ch.E. Journal, **13**, 132, 1967.

20 June 1967

Institute of Heat and Mass Transfer, AS BSSR, Minsk